Bioorganic & Medicinal Chemistry 17 (2009) 6952–6958

Contents lists available at ScienceDirect

Bioorganic & Medicinal Chemistry

journal homepage: www.elsevier.com/locate/bmc

Design of a bioreductively-activated fluorescent pH probe for tumor hypoxia imaging

Eiji Nakata [a,*], Yoshihiro Yukimachi [a], Hirokazu Kariyazono [a], Seongwang Im [a], Chiaki Abe [a], Yoshihiro Uto [a], Hiroshi Maezawa [b], Toshihiro Hashimoto [c], Yasuko Okamoto [c], Hitoshi Hori [a,*]

[a] Department of Life System, Institute of Technology and Science, Graduate School, The University of Tokushima, Minamijosanjimacho 2, Tokushima 770-8506, Japan
[b] Faculty of Medicine, The University of Tokushima, Tokushima 770-8509, Japan
[c] Faculty of Pharmaceutical Sciences, Tokushima Bunri University, Yamashiro-cho, Tokushima 770-8514, Japan

ARTICLE INFO

Article history:
Received 16 June 2009
Revised 6 August 2009
Accepted 7 August 2009
Available online 21 August 2009

Keywords:
Fluorescent pH probe
Tumor hypoxia
Fluorescent imaging
Bioreductive activation
Nitro reduction

ABSTRACT

We have designed and evaluated UTX-12 as a novel fluorescent pH probe for tumor hypoxia imaging. UTX-12 consists of a *p*-nitro benzyl moiety, which is a latent hypoxia-selective leaving group activated by nitro reduction, directly linked to SNARF. Although UTX-12 itself is colorless and non-fluorescent in aqueous solution, nitro reduction triggers the release of SNARF which has well-characterized long wavelength absorption and fluorescence that is sensitive to pH. The resultant SNARF, released intracellularly by enzymatic reduction of UTX-12, allows measurement of pH by pH-dependent dual emission shifts. UTX-12 showed clear differences in fluorescence behavior between hypoxic and aerobic conditions in liver microsomes and inside V79 cells. These data are confirmation that UTX-12 is biologically reduced inside tumor cells and the released SNARF should monitor intracellular pH of tumor cells selectively with reduced background signal.

1. Introduction

Robust tumor growth requires the presence of a local vascular network that supplies both oxygen and nutrients to tumor cells. However, a highly proliferative mass of tumor cells develops faster than the vasculature, and new tumor cells are formed with an avascular environment deficient in oxygen, a condition known as tumor hypoxia. Tumor hypoxia is characterized by low oxygen tension, low nutrient level, low pH and an over-expression of angiogenic factors. This is a fundamentally important character of the tumor environment because it has been associated closely with the malignant phenotype of cancer disease, resistance to cancer therapies, and the high mortality rate of cancer patients.[1,2] For these reasons the specific characteristics of tumor hypoxia are attractive targets in the development of anticancer drugs.[3–6] In addition, there has been an increasing clinical interest in hypoxia-specific molecular probes which can characterize the hypoxic cells fraction before, during and after therapy.[7]

To measure tumor oxygenation in experimental or clinical tumors, different analytical probes have been used in various methods.[8,9] Among these, fluorescent detection has several advantages including high resolution, high sensitivity and noninvasiveness.[7,10] Included in this approach are a few examples of a strategy to identify hypoxic cells by using fluorescent probes which become more fluorescent after biological reduction resulting from tumor hypoxia.[11–16] Although these are promising candidates as tumor hypoxia-selective fluorescent probes, there are two drawbacks. The first is that the maximal absorption wavelength of most of the fluorescent probes used in this approach is less than 500 nm, a complication for bio-imaging because there are many biomolecules that absorb at such a short wavelength. In general, fluorophores with long absorption and fluorescence wavelengths are more suitable as fluorescent probes for in vivo usage. The second drawback is that all of these fluorescent probes were activated irreversibly under hypoxic conditions, a factor that could possibly complicate the monitoring of any time-dependent change during therapy. The fluorescent probe which has a reversible functionality would be more useful because it would have the potential to monitor the therapeutic effect in real time.[17] These considerations prompted us to investigate the design of a fluorescent pH probe which would be selectively and irreversibly activated under tumor hypoxia and subsequently able to monitor the pH in its local environment reversibly, an important determination since pH measurements in tumors have significant diagnostic value.[18,19] Thus, tumor cells have a very high capacity to produce lactic acid, which is generated through glucose metabolism and inefficient vascular clearing, resulting in an acidic microenvironment in solid

* Corresponding authors. Tel./fax: +81 88 656 7517 (E.N.); tel.: +81 88 656 7514; fax: +81 88 656 9164 (H.H.).
E-mail addresses: nakata@bio.tokushima-u.ac.jp (E. Nakata), hori@bio.tokushima-u.ac.jp (H. Hori).

0968-0896/$ - see front matter © 2009 Elsevier Ltd. All rights reserved.
doi:10.1016/j.bmc.2009.08.037

tumors.[1,2] Therefore, the monitoring of tumor pH plays a significant role in cancer treatment.[20–25] In this article, we describe the design and synthesis of new fluorescent pH probes to detect tumor hypoxia selectively and to monitor the pH of the tumor in a reversible manner.

2. Results and discussion

2.1. Molecular design and synthesis

UTX-12 was designed as the hypoxia-selective fluorescent pH probe. This molecule is comprised of a *p*-nitrobenzyl moiety directly linked to SNARF (seminaphthorhodafluors) through an ether linkage (Fig. 1). SNARF belongs to the group of asymmetric xanthene derivatives which are well known as long-wavelength fluorophores. It is, in particular, an example of a pH indicator that shows a dual-emission change (typically 583 nm and 627 nm) in the neutral pH region (pK_a = 7.5). It is therefore useful for measuring pH changes around the physiological pH range (pH 6.5–8.5).[26] In our strategy, the phenolic substituent of SNARF, which is the critical substituent responsible for the unique fluorescent properties, was masked by the nitro benzyl moiety. This moiety is often used as the leaving group activated by biological reduction in hypoxia-selective prodrug strategies.[5,6] As depicted in Figure 2, the nitro benzyl moiety is reduced via a series of one-electron reduction processes to form the hydroxylamino ($4e^-$) and amino ($6e^-$) intermediates that lead to the release of SNARF. However the radical anion product of the first electron reduction step is re-oxidized efficiently to UTX-12 in the presence of oxygen, making further reduction dependent on hypoxic conditions. This selective reduction of the nitro benzyl moiety under hypoxia is the key to giving UTX-12 the potential of being a hypoxia-selective fluorescent pH probe (Fig. 2). UTX-38 was designed as a control compound that is lacking the nitro substituent on the benzyl moiety (Fig. 1). The synthetic routes to UTX-12 and UTX-38 are shown in Scheme 1. As shown, treatment of SNARF with excess K_2CO_3 and *p*-nitrobenzyl bromide or benzyl bromide in dry DMF gave UTX-12 or UTX-38, respectively.

2.2. Spectral analysis

We first compared the absorption and the fluorescence spectrum of UTX-12 and UTX-38 with that of the reference compound SNARF (Fig. 3). SNARF produced maximal absorption and strong fluorescence at 544 nm and 583 nm (λ_{ex} = 534 nm), respectively. In contrast, UTX-12 and UTX-38 displayed no significant absorption above 400 nm and no fluorescence excitation at 534 nm. The corresponding values of λ_{max}, extinction coefficient at λ_{max} (ε), λ_{em}, and quantum yield (ϕ) at pH 5.0 are listed in Table 1. The relative intensities of these compounds were determined by calculating the product of extinction coefficient and quantum yield and then normalizing these values to those of SNARF. These values also are given in Table 1.[26] As compared to SNARF, UTX-38 had only 1.6% and UTX-12 had less than 0.5% of the intensity of SNARF. It is well known that SNARF exists as an equilibrium mixture of the quinoid form that absorbs visible light and is fluoresce and the lactone form that is colorless and non-fluorescent.[26,27] The absorption and fluorescent spectral data indicate that UTX-12 and UTX-38 exist mainly as the lactone form in aqueous solution and that the fluorescence of UTX-12 is also quenched by the nitro group, a well known quencher of fluorophores.[11–14]

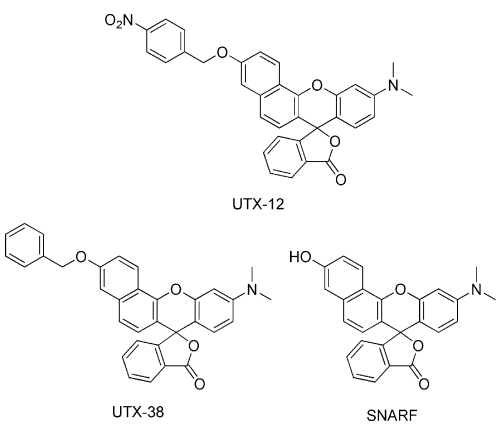

Figure 1. The structure of UTX-12, UTX-38 and SNARF.

2.3. Nitro reduction of UTX-12 catalyzed by nitroreductase

To test the selective deprotection of UTX-12 via nitro reduction, enzymatic reduction of the *p*-nitrobenzyl moiety was carried out using nitroreductase from *Escherichia coli* (NTR), an example of an oxygen-insensitive nitroreductase.[28] When the absorption spectrum and fluorescent spectrum of UTX-12 were measured in the NTR, a time dependent absorption and fluorescence increase originating from SNARF was observed (Fig. 4a and b). The conversion yield (95%) from UTX-12 to SNARF and the maximal fluorescence change (40 times) after 6 h treatment were determined by the absorption spectrum and fluorescence spectrum, respectively. In contrast, no SNARF fluorescent increase was observed in the absence of NTR (Fig. 4c). In addition, no increase was observed using UTX-38 instead of UTX-12 (Fig. 4c). The decrease of UTX-12 and production of SNARF were confirmed by HPLC analysis (Fig. S-1). All of these results indicate that the reduction of the nitro substituent of the *p*-nitro benzyl moiety triggered the release SNARF from UTX-12. To demonstrate the property of pH response of UTX-12 after biological reduction of the nitro substituent, the UTX-12 solution prepared with or without NTR in different pH conditions (pH 5.0, pH 7.0, pH 9.0) were observed by using a transilluminator and the fluorescent spectrometer. The dependence of fluorescent enhancement by nitro reduction and fluorescent color change on the pH was confirmed (Fig. 4d). Based on these data, UTX-12 was demonstrated to function as a fluorescent pH probe mediated by nitro reduction.

2.4. Biological reduction of UTX-12 under different oxygen concentrations

To further evaluate the potential of the UTX-12 as a hypoxia-selective pH probe, we used fluorescence to monitor its biological reduction in different oxygen concentrations. Preparations of liver microsomes of chick embryo were used as a metabolic enzyme cocktail. This includes cytochrome P450 reductase, an electron-donating protein that catalyzes the one-electron reduction of nitro derivatives to nitro anion radicals.[29–31] UTX-12 was incubated with the microsomes in different oxygen concentrations, including hypoxic (without oxygen), aerobic (20% v/v) and oxic conditions (95% v/v), respectively. The time course of fluorescent spectral change under hypoxic conditions is shown in Figure 5a. Intense fluorescence emission originating from SNARF and its time dependent increase (sixfold after 20 h incubation) were observed (inset of Fig. 5a). In contrast, under both aerobic and oxic conditions after 20 h incubation, the extent of enhanced fluorescence intensity diminished significantly as a result of the competitive scavenging by molecular oxygen (Fig. 5b and inset). The hypoxic-aerobic or oxic fluorescence differential became almost five to sixfold after 20 h incubation. As measured by HPLC (Fig. S-2), the differences in the fluorescence intensities of these samples correlate well with

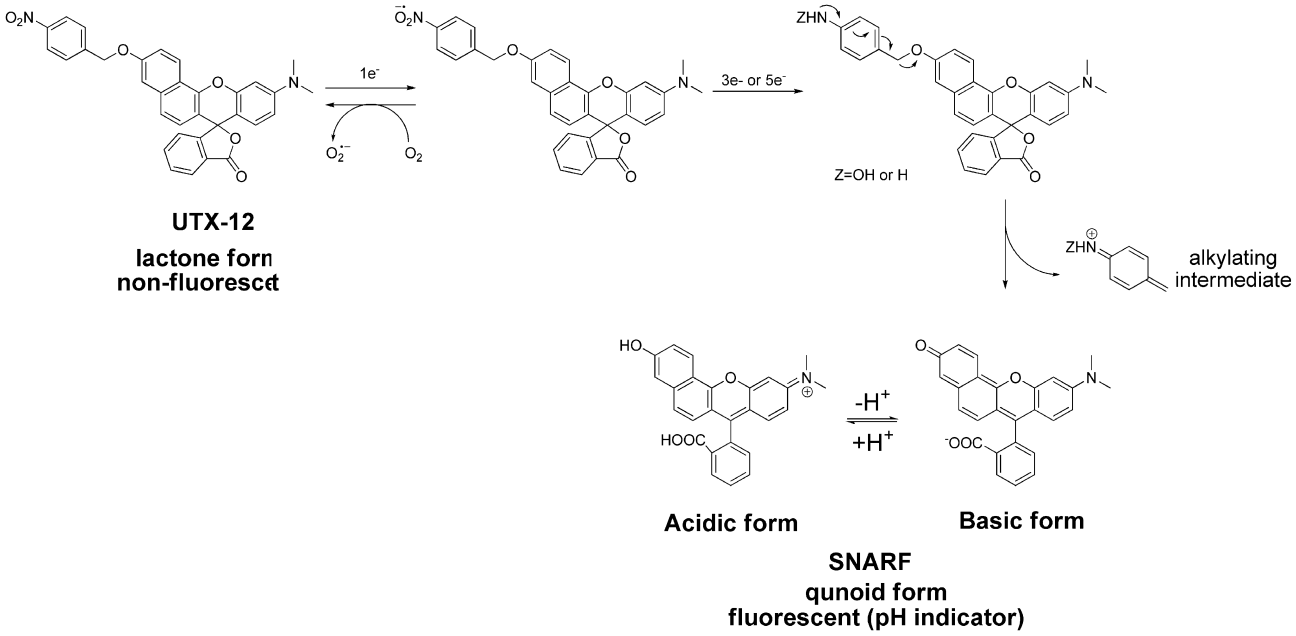

Figure 2. Presumed reaction schemes of UTX-12 as the fluorescent pH probe activated under hypoxia.

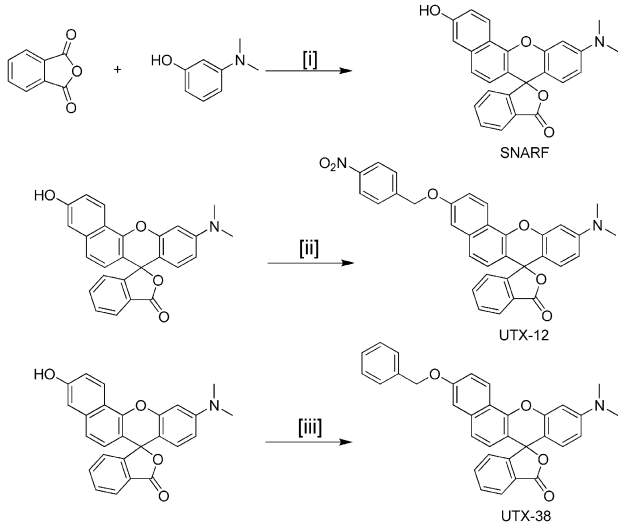

Scheme 1. Synthesis of SNARF, UTX-12 and UTX-38. Reagents and conditions: (i) (1) toluene, reflux; (2)1,6-dihydroxynaphthalene, $ZnCl_2$, 160 °C; (ii) *p*-nitrobenzylbromide, K_2CO_3, dry DMF, rt; (iii) benzylbromide, K_2CO_3, dry DMF, rt.

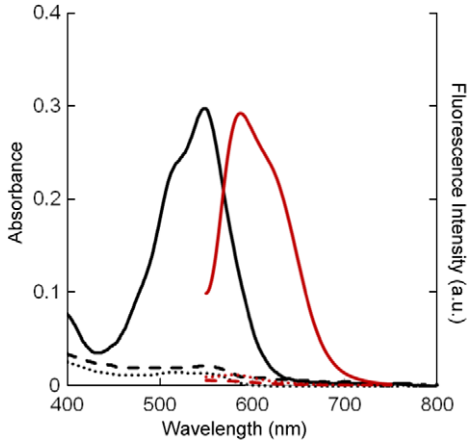

Figure 3. Absorption (black) and emission (red) spectra of SNARF derivatives at pH7.0 used in this study. (solid line: SNARF, dashed line: UTX-12, dotted line: UTX-38).

the hypoxia-selective release of SNARF from UTX-12 upon treatment with the liver microsomes of chick embryo. This indicates that UTX-12 is stable to other metabolizing enzyme in liver microsomes which function independent of oxygen concentration. This is an important requirement for hypoxia-activated fluorescent probes in order to reduce background signal. All of these results demonstrated that UTX-12 was reduced and SNARF was produced under hypoxic conditions, selectively.

2.5. Fluorescent imaging of hypoxic cell by using UTX-12

To further assess the potential applications of UTX-12, fluorescent imaging inside the hypoxic cell using UTX-12 was examined. V79 cells (Chinese hamster lung) were incubated with UTX-12 under hypoxic or aerobic conditions, respectively. After exchanging medium, confocal laser scan microscopy (CLSM) was performed. As shown in Figure 6a, strong fluorescence in the cytosol of V79 cells which were incubated under hypoxic conditions was observed. In contrast, negligible fluorescence was observed in the cells treated under aerobic conditions (Fig. 6b). Figure 6c shows the time-course of fluorescence intensity of UTX-12 incubated under different conditions. The hypoxic-aerobic fluorescent differential increased fourfold after incubation for 6 h.[32] These results indicate that UTX-12 responds to the oxygen concentration and that UTX-12 has a potential to use as a fluorescent pH probe in cell.

3. Conclusion

In this study, we have demonstrated the design and evaluation of a novel fluorescent pH probe for tumor hypoxia. SNARF, which has long wavelength fluorescence emission and has the potential to monitor pH in neutral range, was released from UTX-12 after ni-

Table 1
Spectroscopic properties of SNARF, UTX-12 and UTX-38

Compounds	λ_{max}^{Abs} ($\varepsilon \times 10^{-3}$) [a] (nm) ($M^{-1}$ cm^{-1})	λ_{max}^{Em} (nm)[b]	Φ ($\times 10^{-2}$)	$\varepsilon \times \phi$ (rel)
SNARF[c]	515 (17.7) 544 (21.6)	583	3.0	100%
UTX-12	520 (2.07) 545 (1.82)	—[d]	—[d]	<0.5%
UTX-38	520 (2.16) 545 (1.88)	579	0.5	1.6%

[a] Measured in pH 5.0 10 mM acetate buffer.
[b] Excited at 534 nm.
[c] Ref. 26.
[d] Precise values cannot be determined because of low fluorescence.

tro reduction. The selective biological reduction under tumor hypoxic conditions and release of SNARF thus enable UTX-12 to be used to measure the proximal pH of the tumor. Furthermore, UTX-12 produced a clear fluorescence differential between hypoxic and aerobic conditions in the liver microsomes of chick embryo and inside V79 cells. Based on these data, we conclude that UTX-12 can produce fluorescence under tumor hypoxia selectively and should monitor the pH of tumor hypoxia reversibly.

To describe the tumor pH environment in detail, the extracellular fluid of tumor cells is acidified (pH 6.2–6.8; pH_e) in order to maintain the intracellular pH (pH_i) at a relatively normal pH (pH 7.0–7.4). This condition is reported to result from hypoxia inducible factor (HIF) mediated up-regulation and activation of a number of membrane located transporters, exchanges, pumps and ecto-enzymes.[18] Inhibiting such selectively up-regulated functions in tumor cells, for example, carbonic anhydrase IX which is a high activity tumor-associated membrane enzyme predominantly found in hypoxic tumor tissues and is absent from most normal tissues, may suffice to allow acidic metabolites to build up intracellularly within a tumor and inhibit proliferation. Thus, acidic pH_i has been shown to affect cell function, growth and division, and can be clastogenic and even induce apoptosis.[19,22] For the purpose of anticancer drug development based on this strategy, selective pH_i measurement in tumor cells would be very useful for high throughput screening and direct monitoring of the effect of an anticancer drug.

In summary, we have demonstrated that UTX-12 can be selectively activated by reductive enzymes under the conditions of tumor hypoxia. This activation in turn triggers to release SNARF inside tumor cells where it should monitor the pH_i selectively with reduced background signal. Although SNARF derivatives have previously been used to monitor intra- or extracellular compartments for different purposes,[22,23] we note that UTX-12 is the first example of selective translocation of SNARF as a fluorescent pH probe into tumor cells. On these points, we believe that UTX-12 should be a promising candidate for further evaluation as a fluorescent pH probe for tumor hypoxia in vivo. In addition to monitoring the oxygen environment, potential applications include following the effects of drug treatment through pH_i measurement.

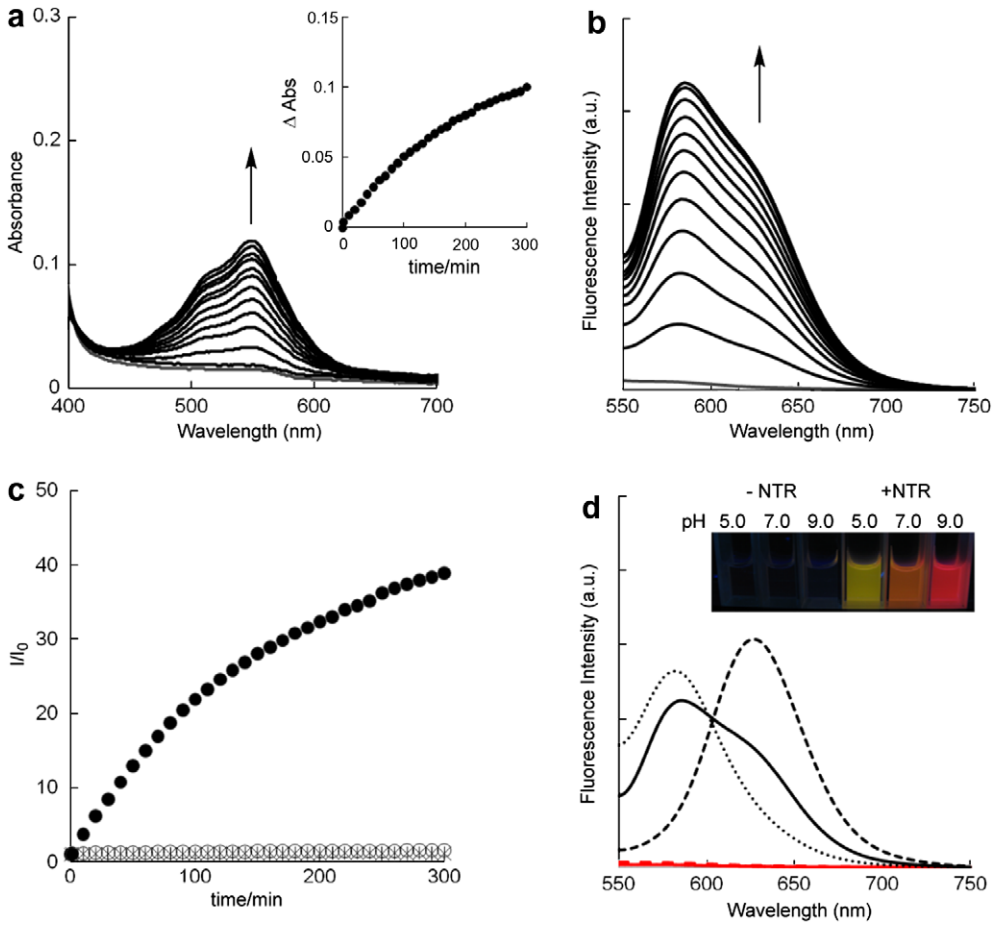

Figure 4. (a and b) Real time spectral change of NTR-catalyzed nitro reduction. (a) Absorption spectral change. (b) Fluorescence spectral change. (c) Time profile of the relative emission intensity (black circle: UTX-12 with NTR, white circle: UTX-38 with NTR, asterisk: UTX-12 without NTR). (d) The fluorescence spectra of UTX-12 in the presence (black) or absence (red) of NTR in pH 5.0 (dot line), pH 7.0 (solid line) and pH 9.0 (dashed line), respectively. Inset: Photograph of the ratiometric fluorescent response in different pH conditions with or without NTR.

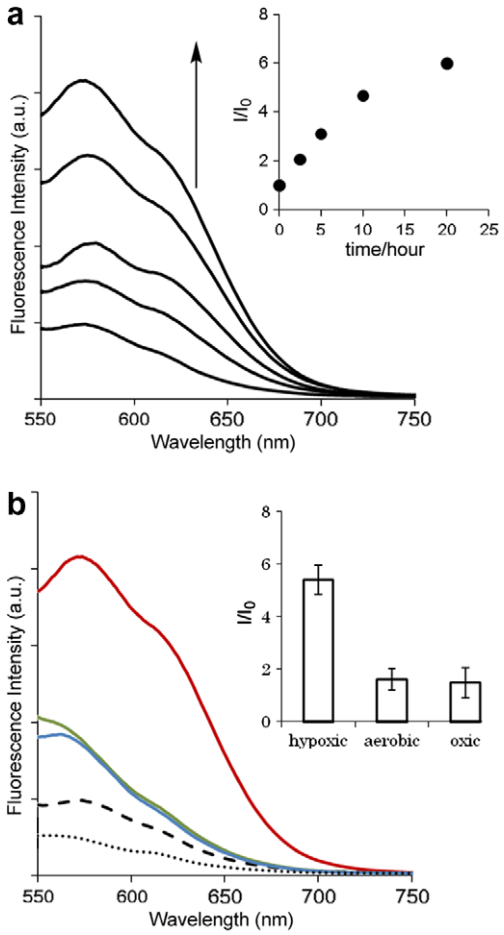

Figure 5. (a) The spectral change of the UTX-12 incubated with liver microsomes of chick embryo under hypoxic condition at different incubation times (0, 2.5, 5, 10 and 20 h). Inset: time profile of the relative emission intensity (λ_{em} = 627 nm) caused by incubation under hypoxic conditions. (b) Fluorescence spectra of UTX-12 resulting from incubation under different oxygen concentration. (solid line: UTX-12 was incubated with liver microsomes for 20 h under hypoxic (red), aerobic (green) and oxic (blue) conditions, dashed line (black): UTX-12 was incubated with liver microsomes for 0 h, dotted line (black):UTX-12 in 0.1 M phosphate buffer (pH 7.4) without liver microsomes. Inset: The relative emission intensity of UTX-12 (λ_{em} = 627 nm) incubated in the different oxygen concentration.

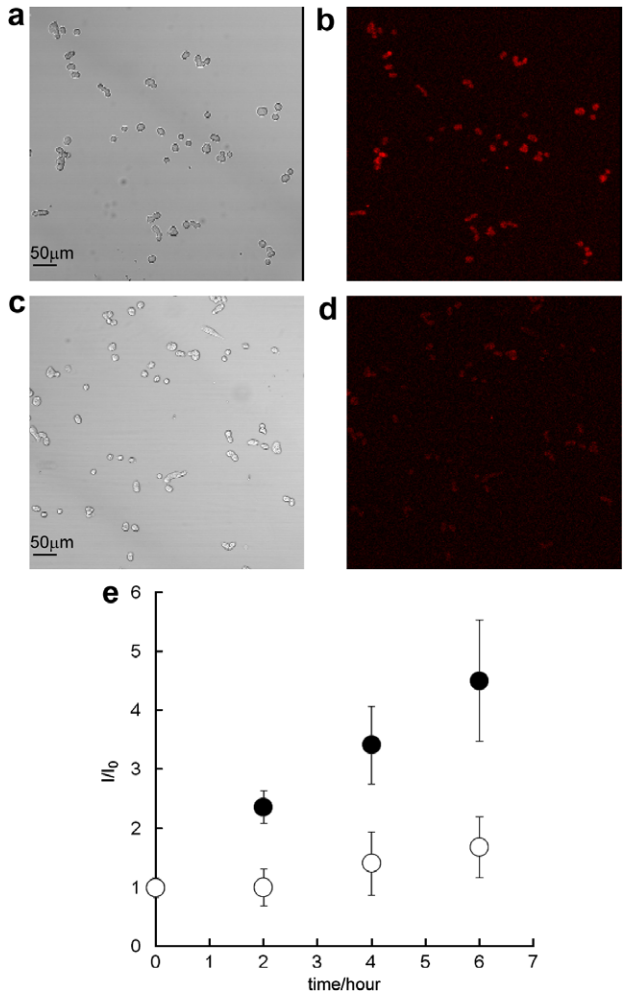

Figure 6. (a–d) Fluorescence microphotograph of V79 cells incubated with UTX-12 for 6 h under (a and b) hypoxic conditions (incubated in 95% N_2 and 5% CO_2) or (c and d) aerobic conditions (incubated under atmosphere gas). (a and c) Transmission channel. (b and d) fluorescence channel. The scale bar (50 μM) are shown in the photograph. (e) The time courses of accumulation of fluorescent intensity in V79 cells incubated with UTX-12 under hypoxic (●) or aerobic (○) conditions.

4. Experimental

4.1. General procedures

^{1}H NMR spectra were recorded on JEOL JNM-EX400 spectrometer (400 MHz) with tetramethylsilane as the internal standard. Chemical shifts are reported in ppm. Coupling constants are reported in Hz. IR spectra were measured in KBr pellets with a Perkin–Elmer 1600 spectrometer. HRMS were measured on a JOEL JMS-700 mass spectrometer using the FAB method. Elemental analyses were performed with a Yanako CHN recorder MT-5. Reactions were monitored by analytical TLC using Merck Silica Gel 60 F_{254} aluminium plates. Column chromatography was performed on Kanto Chemical Silica Gel 60 N (230–400 mesh). Absorption spectra were recorded on a Hitachi U3300 spectrometer. Fluorescent spectra were recorded on a Hitachi F-4500 spectrometer. HPLC was performed on a μRPC C2/C18 SC column (2.1 × 100 mm, Pharmacia) with a Pharmacia Biotech SMART system. All chemicals were purchased from Wako Pure Chemical Industries, Ltd (Osaka, Japan), Kanto Chemical Co., Inc. (Tokyo, Japan), Tokyo Chemical Industry Co., Ltd (Tokyo, Japan), or Sigma–Aldrich Japan (Tokyo, Japan).

4.2. Synthesis

10-(Dimethylamino)-3-hydroxy-Spiro[7*H*-benzo[*c*]xanthene-7,1′(3′*H*)-isobenzofuran]-3′-one (seminaphthorhodafluor, SNARF) was synthesized according to the literature procedure.[33,34]

4.2.1. 10-(Dimethylamino)-3-[(4-nitrophenyl)methoxy]-spiro-[7*H*-benzo[*c*]xanthene-7,1′(3′*H*)-isobenzofuran]-3′-one (UTX-12)

A mixture of SNARF (58.2 mg, 142 μmol), K_2CO_3 (68.5 mg, 496 μmol), 4-nitrobenzyl bromide (50.3 mg, 233 μmol) in dry DMF (2.5 ml) was stirred for 6.5 h at room temperature. The reaction mixture was diluted with CH_2Cl_2 and washed with satd $NaHCO_3$ aq followed by drying over anhydrous Na_2SO_4. The solvent was removed in vacuo, and the residue was purified by column chromatography on silica gel (CH_2Cl_2/AcOEt: a linear gradient from 1:0 to 1:1(v/v)) to give UTX-12 as a pale pink powder in 40% yield (30.6 mg):^{1}H NMR ($CDCl_3$, 400 MHz): δ_H 8.54 (d (9.3 Hz),1H, Ar–*H*), 8.27 (d (8.8 Hz), 2H, Ar–*H*) 8.05 (dd (6.2, 1.6 Hz), 1H, Ar–*H*), 7.59–7.68 (m, 4H, Ar–*H*), 7.36 (dd (9.1, 2.3 Hz), 1H, Ar–*H*), 7.30 (d (8.8 Hz), 1H, Ar–*H*), 7.14–7.15 (m, 2H, Ar–*H*), 6.74 (d (8.8 Hz), 1H, Ar–*H*), 6.67–6.70 (m, 2H, Ar–*H*), 6.48 (dd (8.9, 2.6 Hz), 1H, Ar–*H*), 5.30 (s, 2H, Ar–*CH*$_2$-Ar), 3.03 (6H, s, N–*CH*$_3$) FT-IR(KBr) 3478,

3079, 2911, 1749, 1627, 1521, 1419, 1361, 1344, 1250, 1110, 852 cm^{-1}; FAB-HRMS (*m*-NBA): calcd for $C_{33}H_{25}N_2O_2^+$ ($[M+H]^+$) 545.1713, found 545.1729. Anal. Calcd for $C_{33}H_{24}N_2O_6$: C, 72.78; H, 4.44; N, 5.14. Found: C, 72.55; H, 4.61; N, 5.12.

4.2.2. 10-(Dimethylamino)-3-phenylmethoxy-Spiro[7*H*-benzo[*c*]xanthene-7,1′(3′*H*)-isobenzofuran]-3′-one (UTX-38)

A mixture of SNARF (50.9 mg, 124 μmol) K_2CO_3 (60 mg, 434 μmol), benzyl bromide (29.5 μl, 248 μmol) in dry DMF (2 ml) was stirred for 19 h at room temperature. The reaction mixture was diluted with CH_2Cl_2 and washed with satd $NaHCO_3$ aq followed by drying over anhydrous Na_2SO_4. The solvent was removed in vacuo, and the residue was purified by column chromatography on silica gel (CH_2Cl_2 only and then CH_2Cl_2/MeOH = 50:1 (v/v)) to give UTX-38 as a pale pink powder in 76% yield (46.8 mg): ^1H NMR ($CDCl_3$, 400 MHz) δ_H 8.52 (d (9.0 Hz), 1H, Ar–*H*), 8.05 (dd (6.3, 1.7 Hz), 1H, Ar–*H*), 7.58−7.66 (m, 2H, Ar–*H*), 7.49 (d (6.8 Hz), 2H, Ar–*H*), 7.41 (t (6.6 Hz), 2H, Ar–*H*), 7.36 (dd (9.3, 6.8 Hz), 2H, Ar–*H*), 7.31 (d (8.5 Hz), 1H, Ar–*H*), 7.19 (d (2.4 Hz), 1H, Ar–*H*), 7.15 (dd (6.5, 1.3 Hz), 1H, Ar–*H*), 6.72 (d (8.8 Hz), 1H, Ar–*H*), 6.67–6.70 (m, 2H, Ar–*H*), 6.47 (dd (8.8, 2.4 Hz), 1H, Ar–*H*), 5.20 (s, 2H, Ar–*CH*$_2$–Ar), 3.03 (s, 6H, N–*CH*$_3$); FT-IR(KBr) 3430, 2926, 2855, 2365, 1752, 1626, 1422, 1252, 1115 cm^{-1}; FAB-HRMS (*m*-NBA): calcd for $C_{33}H_{26}NO_4^+$ ($[M+H]^+$) 500.1862, found 500.1884. Anal. Calcd for $C_{33}H_{25}NO_4$: C, 79.34; H, 5.04; N, 2.80. Found: C, 79.08; H, 5.29; N, 2.87.

4.3. Spectroscopic assessment

4.3.1. Measurement of extinction coefficients

The extinction coefficients (ε) of UTX-12 and UTX-38 were calculated according to the Lambert–Beer law. Absorption spectra of the samples were measured in pH 5.0 10 mM acetate, HEPES and Tris buffer.

4.3.2. Fluorescence spectrophotometry

Fluorescence spectra of UTX-12, UTX-38 and SNARF were measured with excitation at 534 nm in pH 5.0 or pH 7.0 10 mM acetate, HEPES and Tris buffer at 20 ± 1 °C. The slit widths of the excitation and emission were set to 10 nm and 10 nm, respectively.

4.3.3. Measurement of fluorescence quantum yield

The fluorescence quantum yield (Φ) was determined by integration of corrected emission spectra, compared to a SNARF standard with a known value of 0.03 of the same optical density at 534 nm.[26] Under these conditions, quantum yields were calculated using Eq. 1.

$$\Phi_{\text{sample}} = \Phi_{\text{standard}} \left(\int F_{\text{em, sample}} \Big/ \int F_{\text{em, standard}} \right) \quad (1)$$

4.4. Biological analysis

4.4.1. Bioreductive activation of nitroaromatic residue by nitroreductase

Nitroreductase from *E. coli* (NTR) was purchased from SIGMA co. ltd. The preincubated solution of UTX-12 (5.0 μM) and NADPH (500 μM) in the assay buffer (50 mM Tris–HCl buffer (pH 7.0)) at 20 ± 1 °C was mixed with NTR (final concentration: 0 or 2.0 U/ml). The fluorescence spectrum (excitation wavelength: λ_{ex} = 534 nm) and UV–vis spectrum then was monitored from 0 to 300 min. As the control experiment, UTX-38 (5.0 μM) instead of UTX-12 was used. The conversion yield from UTX-12 to SNARF was calculated by UV–vis spectrum ($\varepsilon_{534\ nm}$ = 25 750 M^{-1} cm^{-1}).

The reaction solutions were analyzed by HPLC after centrifugation. The HPLC solvents employed were 95% acetonitrile and 5% water containing 0.1% trifluoroacetic acid (TFA) (solvent A) and water containing 0.1% TFA (solvent B). HPLC conditions were as follows: solvent A: solvent B = 0:100 (0 min)–0:100 (5 min)–100:0 (55 min), flow rate 200 μl/min, detection by UV (280 nm) (HPLC charts were shown in Supplementary data).

The reaction solution of UTX-12 (50 μM) and NADPH (2 mM), which was incubated with or without NTR (2.0 U/ml) for 22 h under darkness, was adjusted pH 5.0, pH 7.0 and pH 9.0 was observed by using UV transilluminator (Vilber Lourmat TFX-20.M, λ_{ex} = 312 nm) and fluorescence spectrometer.

4.4.2. Bioreductive activation of UTX-12 by microsomes of chick embryo under different oxygen concentration

The liver microsomes were prepared according to the method reported previously with a slight modification.[35] Chick embryo liver microsomes were prepared from a pooled set of fourteen liver samples (4.899 g). After homogenization of the liver samples in three volume of 50 mM phosphate 0.25 M sucrose pH 7.4, microsomes (0.777 g wet weight) were isolated by centrifugation at 10,000*g* and 105,000*g*, and resuspended in 6.0 ml of 0.1 M phosphate buffer pH 7.4. The samples were prepared with microsomes (64.8 mg/ml), UTX-12 (50 μM), NADPH (2 mM) and $MgCl_2$ (3 mM) in 0.1 M phosphate buffer pH 7.4. To establish hypoxic conditions, the suspension was degassed with three freeze-pump-thaw cycles under nitrogen gas (without oxygen). To generate oxic conditions, the suspension was vigorously bubbled for 20 s with a gas mixture containing 95% oxygen and 5% carbon dioxide. For control, similar compositions as in the foregoing samples were prepared without UTX-12 or microsomes, respectively. All these samples were incubated at 37 °C. After the appropriate incubation time (hypoxic conditions: 0, 2.5, 5, 10, 20 h, the others: 20 h), these samples were centrifuged at 105,000*g* and the fluorescent spectra of the supernatants were measured.

The supernatants were diluted with equal amounts of DMSO and were filtered with Millipore Millex-GV filters (pore size 0.22 μM). The filtrates were analyzed by HPLC under the same conditions as described above (detection by UV at 534 nm, HPLC charts are shown in Supplementary data).

4.4.3. Bioimaging of V79 cells incubated under different oxygen conditions by using UTX-12

V79 cells were cultured in Eagle minimum essential medium without phenol red containing 12.5% (v/v) fetal bovine serum and kanamycin (60 mg/l) at 37 °C in 5% CO_2. Cells (5×10^4 cells) in late log phase were seeded in a 35-mm glass base dish. After growth in a CO_2 incubator for 12 h, the culture medium was exchanged to drug containing medium (UTX-12 50 μM). The cells were then placed in a hypoxic chamber flushed with 5% CO_2 and 95% N_2 at 25 °C for 2, 4, 6 h at flow rates of 1.5–2.0 NL/min for hypoxic conditions. For the aerobic conditions they were placed at 25 °C under atmosphere gas. After treatment, the culture medium was exchanged to fresh medium and observed by confocal laser scanning microscopy (CLSM, Nikon C1si-Ready). Fluorescence at the emission wavelength of 605 nm was measured at room temperature by exciting SNARF at 544 nm. The fluorescence intensities of the CLSM images were obtained by the averaged value of at least ten independent points of the photos. The scanning speed and the laser intensity were adjusted to avoid photobleaching.

Acknowledgements

This work was supported in part by Grant-in-Aid for Young Scientist (B) (No. 21710232) from the Ministry of Education, Culture, Sports, Science and Technology, Japan. The authors thank Professor Itaru Hamachi (Kyoto University) for usage of the fluorescent spectra measurement, and Ms. Maki Nakamura, Ms. Yuka Sasaki, Ms.

Emiko Okayama and the staff of our Faculty for measurement of NMR, HPLC and elemental analysis, and Ms. Sayuri Tomonari for support on CLSM measurements. We also thank Dr. Kenneth L. Kirk (NIH) for his critical and valuable comments.

Supplementary data

Supplementary data associated with this article can be found, in the online version, at doi:10.1016/j.bmc.2009.08.037.

References and notes

1. Hanahan, D.; Weinberg, R. A. *Cell* **2000**, *100*, 57.
2. Brahimi-Horn, M. C.; Chiche, J.; Pouyssegur, J. *J. Mol. Med.* **2007**, *85*, 1301.
3. Nagasawa, H.; Uto, Y.; Kirk, K. L.; Hori, H. *Biol. Pharm. Bull.* **2006**, *29*, 2335.
4. Tanabe, K.; Zhang, Z.; Ito, T.; Hatta, H.; Nishimoto, S. *Org. Biomol. Chem.* **2007**, *5*, 3745.
5. Chen, Y.; Hu, L. Q. *Med. Res. Rev.* **2009**, *29*, 29.
6. Jaffar, M.; Williams, K. J.; Stratford, I. J. *Adv. Drug Deliv. Rev.* **2001**, *53*, 217.
7. Benaron, D. A. *Cancer Metas. Rev.* **2002**, *21*, 45.
8. Fyles, A. W.; Miolsevic, M.; Wong, R.; Kavanagh, M. C.; Pintilie, M.; Sun, A.; Chapman, W.; Levin, W.; Manchul, L.; Keane, T. J.; Hill, R. P. *Radiother. Oncol.* **1998**, *48*, 149.
9. Al-Hallaq, H. A.; River, J. N.; Zamora, M.; Oikawa, H.; Karczmar, G. S. *Int. J. Radiat. Oncol. Biol. Phys.* **1998**, *41*, 151.
10. Willmann, J. K.; van Bruggen, N.; Dinkelborg, L. M.; Gambhir, S. S. *Nat. Rev. Drug Discovery* **2008**, *7*, 591.
11. Hodgkiss, R. J.; Jones, G. W.; Long, A.; Middleton, R. W.; Parrick, J.; Stratford, M. R. L.; Wardman, P.; Wilson, G. D. *J. Med. Chem.* **1991**, *34*, 2268.
12. Hodgkiss, R. J.; Middleton, R. W.; Parrick, J.; Rami, H. K.; Wardman, P.; Wilson, G. D. *J. Med. Chem.* **1992**, *35*, 1920.
13. Liu, Y.; Xu, Y. F.; Qian, X. H.; Liu, J. W.; Shen, L. Y.; Li, J. H.; Zhang, Y. X. *Bioorg. Med. Chem.* **2006**, *14*, 2935.
14. Liu, Y.; Xu, Y. F.; Qian, X. H.; Xiao, Y.; Liu, J. W.; Shen, L. Y.; Li, J. H.; Zhang, Y. X. *Bioorg. Med. Chem. Lett.* **2006**, *16*, 1562.
15. Tanabe, K.; Hirata, N.; Harada, H.; Hiraoka, M.; Nishimoto, S. I. *ChemBioChem* **2008**, *9*, 426.
16. Zhu, W. P.; Dai, M.; Xu, Y. F.; Qian, X. H. *Bioorg. Med. Chem.* **2008**, *16*, 3255.
17. Urano, Y.; Asanuma, D.; Hama, Y.; Koyama, Y.; Barrett, T.; Kamiya, M.; Nagano, T.; Watanabe, T.; Hasegawa, A.; Choyke, P. L.; Kobayashi, H. *Nat. Med.* **2009**, *15*, 104.
18. Brahimi-Horn, M. C.; Pouyssegur, J. *FEBS Lett.* **2007**, *581*, 3582.
19. Swietach, P.; Vaughan-Jones, R. D.; Harris, A. L. *Cancer Metas. Rev.* **2007**, *26*, 299.
20. Silva, A. S.; Yunes, J. A.; Gillies, R. J.; Gatenby, R. A. *Cancer Res.* **2009**, *69*, 2677.
21. Chiche, J.; Ilc, K.; Laferriere, J.; Trottier, E.; Dayan, F.; Mazure, N. M.; Brahimi-Horn, M. C.; Pouyssegur, J. *Cancer Res.* **2009**, *69*, 358.
22. Swietach, P.; Wigfield, S.; Cobden, P.; Supuran, C. T.; Harris, A. L.; Vaughan-Jones, R. D. *J. Biol. Chem.* **2008**, *283*, 20473.
23. Gatenby, R. A.; Gawlinski, E. T.; Gmitro, A. F.; Kaylor, B.; Gillies, R. J. *Cancer Res.* **2006**, *66*, 5216.
24. Martin, G. R.; Jain, R. K. *Cancer Res.* **1994**, *54*, 5670.
25. Gallagher, F. A.; Kettunen, M. I.; Day, S. E.; Hu, D. E.; Ardenkjaer-Larsen, J. H.; in't Zandt, R.; Jensen, P. R.; Karlsson, M.; Golman, K.; Lerche, M. H.; Brindle, K. M. *Nature* **2008**, *453*, 940.
26. Whitaker, J. E.; Haugland, R. P.; Prendergast, F. G. *Anal. Biochem.* **1991**, *194*, 330.
27. Lavis, L.; Rains, R. T. *ACS Chem. Biol.* **2008**, *3*, 142.
28. Roldán, M.; Pérez-Reinado, E.; Castillo, F.; Moreno-Vivián, C. *FEMS Microbiol. Rev.* **2008**, *32*, 474.
29. Kupfer, D.; Mani, C.; Lee, C. A.; Rifkind, A. B. *Cancer Res.* **1994**, *15*, 3140.
30. Shephard, E. A.; Phillips, I. R.; Bayney, R. M.; Pike, S. F.; Rabin, B. R. *Biochem. J.* **1983**, *211*, 333.
31. Orna, M. V.; Mason, R. P. *J. Biol. Chem.* **1989**, *264*, 12379.
32. To check the property of released SNARF as the fluorescent pH probe, the incubated V79 cells under hypoxic conditions were lysed and the emission intensity ratio, $R = I_{583\ nm}/I_{627\ nm}$, in whole cell lysate was determined by fluorescent spectrometer (the detail of the preparation are shown in the Supplementary data). The value ($R = 0.84 \pm 0.01$) was calibrated by standard curve (Fig. S-3) and calculated pH was determined (pH = 7.51 ± 0.01). It was in good agreement with the observed pH value (pH = 7.5 ± 0.1).
33. Honda, K.; Nakata, E.; Ojida, A.; Hamachi, I. *Chem. Commun.* **2006**, 4024.
34. Nakata, E.; Wang, H.; Hamachi, I. *ChemBioChem* **2008**, *9*, 25.
35. Toennes, S. W.; Thiel, M.; Walther, M.; Kauert, G. F. *Chem. Res. Toxicol.* **2003**, *16*, 375.